Chemical Physics 393 (2012) 123–128

Contents lists available at SciVerse ScienceDirect

Chemical Physics

journal homepage: www.elsevier.com/locate/chemphys

Ring formation mechanism of single-walled carbon nanotubes: Energy conservation between curvature elasticity and inter-tube adhesion

C.R. Chang [a,b,c], L.H. Lu [a,c], J.H. Liu [a,c], W. Chen [a,*]

[a] Suzhou Institute of Nano-tech and Nano-bionics, CAS, i-lab, Suzhou 215123, China
[b] Institute of Semiconductors, CAS, Beijing 100049, China
[c] Graduate University of the Chinese Academy of Science, CAS, Beijing 100049, China

ARTICLE INFO

Article history:
Received 14 April 2011
In final form 29 November 2011
Available online 14 December 2011

Keywords:
Single-walled carbon nanotubes (SWNTs)
Rings
Elastic
van der Waals (vdW) attractions

ABSTRACT

Rings of single-walled carbon nanotubes (SWNTs) exist widely during water evaporation from their dispersions at low concentration on such substrates as silica wafer. We examine the phenomenon in terms of energy conservation between the increased significant curvature energy and the inherent inter-tube van der Waals (vdW) attraction potentials. And thereby, the observed multi ring structures for coarse and long SWNT bundles have also gained detailed interpretation. We conclude that carbon nanotubes (CNTs) coil into rings by their own elastic mechanism. The formed rings with different width and diameters originate from appropriate sizes of SWNTs or the bundles. Specially, the associated elasticity may have prospective potentials to reveal other fascinating self-assembling phenomenon on CNTs, for instance, the known liquid crystallinity of them. Besides, we have also analyzed the external factors to the ring formation, both statistically and dynamically.

1. Introduction

CNTs are known to be the strongest and the most flexible molecular material and can be found in various configurations and geometries, for instance, nano springs or coils [1–3], self-folded tennis-racket-like structures [4–7] as well as nano rings [8–13]. These alternative forms of carbon are interesting and potentially promising in future nanotechnology if the formations can be reasonably controlled. As works have shown [5,6], studies of such variant carbon structures are expected to help designing nano-scale devices. The related mechanism among them could be integrated and it is important to further understand the response of CNTs to external actions. Because SWNTs consist of only a single graphite layer, they differ from multi-walled carbon nanotubes (MWNTs) and have lower bending rigidity. So generally they are more readily to exist in various shapes and have fewer deformation-induced defects on their walls. Additionally, SWNTs are usually found in bundles of nearly parallel tubules due to the inter-tubular extremely strong vdW attractions, which also partially accounts for the structural complexity. These carbon forms are predicted to be energetically and thermodynamically stable. Within the elasticity theory, it is indicated that there exists the critical curvature radius for defect-free bent CNTs [14]. The occurrence of defects beyond the critical range will allow the relaxation of the strain energy, which is common in MWNT structures. When much smaller curvatures are formed, both SWNTs and MWNTs will be unstable, since the strain energy has exceeded the binding energy of the graphitic network and bond-breaking occurs. Hence, the mechanical properties of CNTs deserve to receive considerable interest and the issue will play important roles in the future CNT-based nano devices.

Here is based upon experimental observations, we provide a theoretical method to explore the formation mechanism of SWNT rings. As frequently seen in DNA [15], these SWNT ring structures should also be mechanically stable both from experimental and theoretical points of view. Therefore in the subsequent sections, we will consider the nanotube bending strain energy and the vdW attraction potentials between different tubes or different parts of them to analyze the observed intriguing ring-forming behavior.

2. Experimental

Raw CNTs were obtained from the Chengdu Organic Chemicals Co. Ltd., Chinese Academy of Science, synthesized by a Chemical Vapor Deposition (CVD) method. CNTs were initially treated in ~40% (wt.%) nitric acid for ~48 h following the typical purification method [16], and then after multiple filtration, redispersion and centrifugation, redissolved in deionized water, forming stable suspensions of CNT concentration ~0.1 mg/ml. The well dispersed CNTs were mostly micrometer long.

* Corresponding author. Address: Dushu Lake Higher Education Town, Ruoshui Road 398, Suzhou Industrial Park, Suzhou. Tel.: +86 512 6287 2528 (O); fax: +86 512 6287 2553.
E-mail address: wchen2006@sinano.ac.cn (W. Chen).

0301-0104/$ - see front matter © 2011 Elsevier B.V. All rights reserved.
doi:10.1016/j.chemphys.2011.11.036

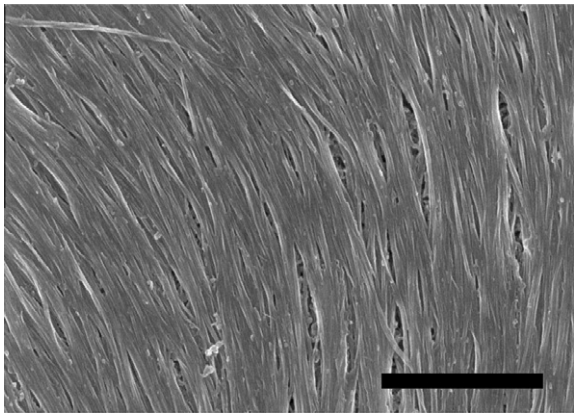

Fig. 1. Scanning electron microscope (SEM) image of the sample from SWNT dispersions, showing that aligned SWNTs lie in the upper layer and the smaller unwanted sphere-like impurity particles lie in the lower layer. The scale bar expresses 1 μm.

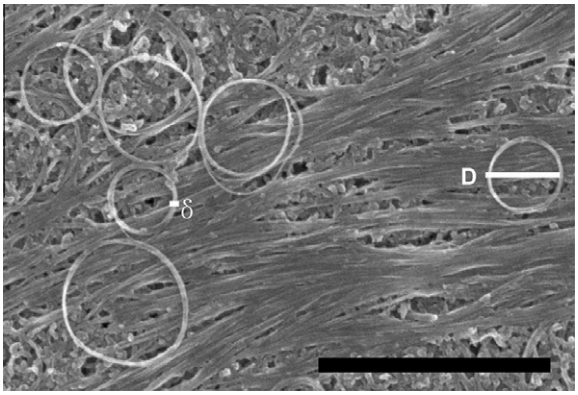

Fig. 2. SEM image of the ring formation from SWNTs or the bundles on top side, and ordered SWNT-assemblies lie in the middle, as well as the impurity particles locate in the lowest layer. Letter D means the diameter of the formed rings and δ refers to their width. The scale bar expresses 1 μm.

The experiments were conducted using the above stable suspensions. Desired volume of the suspension on the microliter scale (e.g., 2.5 μl) was dropped onto a weakly hydrophilic silicon substrate (contact angle between 60° and 90°) and then left to slowly evaporate and concentrate at room temperature for days. As a result, SWNT assemblies in the last deposit are either in the liquid crystalline state, including the existence of liquid crystalline defects (Fig. 1) or in the various self-folding structures (Fig. 2).

However, as is seen in Figs. 1 and 2, even after repeated centrifugation and washing steps, there still exists a high fraction of roughly spherical nanoparticles. They are either integrated into aligned SWNT domains (nematic), or tend to mostly concentrate on the lower sample surface (seeing Fig. 1, under the aligned SWNTs). So, we were determined to explore the self-organizing behavior of dispersions of SWNTs in the presence of such impurities. Maybe, it is the surrounding impurity particles that facilitate and serve to stabilize the alignment of SWNTs at the unexpected low concentrations, with evident rod-rich and sphere-rich areas.

More compellingly, from Fig. 2, quite a number of SWNTs are in the form of rings. On this phase behavior of nanotubes, few theoretical or experimental studies are performed. Thus in the following, we will discuss this interesting phenomenon, and the involved mechanical elastic properties of nanotubes will be introduced.

3. Theoretical

First of all, we assumed that the ring structure is resulted from a coiling process, and then we explore the detailed internal properties of SWNT rings with theoretical models.

Recently, Zhou et al. [17] proposed a method to calculate the strain energies in bent SWNTs (without pentagon–heptagon defects on their walls) by taking account of the total energy of all the occupied band electrons. Because of the similarities with our experiments, we now consider this kind of bending strain energy $\Delta\varepsilon_b$ as follows:

$$\Delta\varepsilon_b = \lambda/R^2 \tag{1}$$

where R is the bending radius and the quantity λ is given by

$$\lambda \approx b * \rho^2 \tag{2}$$

where ρ expresses the radius of a single tube, and b^* is equal to 15.3 eV/atom, describing the energy contribution per carbon atom in SWNTs.

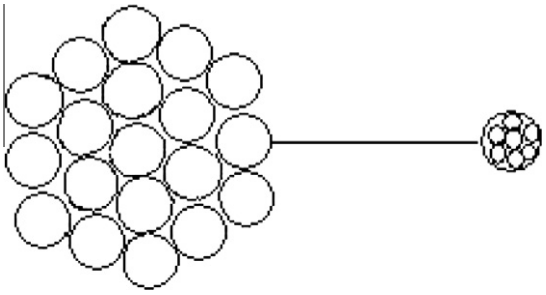

Fig. 3. Hexagonal close-packed structure for the cross section of the formed rings (left) and of the original SWNT bundles (right). Both of them result from the intrinsic vdW attraction interactions between CNTs or the bundles.

Here, in Eq. (2), we have ignored the lower energy contribution from the part of ρ-independence (as described in [17]). However, the following qualitative discussion shows that this point is not the key to account for the variety of SWNT rings that have been observed in experiments.

Further combining the modified vdW interactions for the common SWNT bundles, the attraction potential suggested in [18] takes the form:

$$\varepsilon_{vdW}(\rho) = -0.1135\rho^{1/2} + 9.39 \times 10^{-3} \tag{3}$$

which is the energy of interaction in eV/Å. We assume the bundles consisting of parallel tubes, exhibiting the hexagonal section and then can further align in larger hexagonal structures (seeing the model in Fig. 3). Different CNTs, different nanotube bundles or different parts of them attract each other due to the intrinsic vdW attractions. It is believed that the introduced model will shed light on such ring-structural formation. However, it should be pointed out that, in the model we have neglected the nearest inter tube distance for CNT bundles (about 0.34 nm, right in Fig. 3) and the nearest inter bundle distance (left), given by

$$R_0(\rho) = 2.00\rho + 3.13 \text{ Å} \tag{4}$$

For ρ = 10 Å, there is R_0 = 23.13 Å.

According to the model we consider the total energies for bending strain and the vdW interactions, Eqs. (1) and (3) can then be rewritten as:

$$\Delta E_b = N \cdot \lambda/R^2 \tag{5}$$

$$E_{vdW} = 2\pi R \times \varepsilon_{vdW} \times n_{contact} \tag{6}$$

In Eq. (5), N is the total carbon atom number, given by

$$N = S \cdot \sigma \tag{7}$$

where S is the gross carbon network area in one observed ring, with $S = 2\pi\rho \cdot l$ ($l = 2\pi R \times n_{ring} = 6.28R \times n_{ring}$, n_{ring} is the total number of internal single SWNT rings) and the surface density σ of carbon atoms is assumed to be uniform with $\sigma = 4/(1.732a^2)$, in which $a = 2.49$ Å is the graphene lattice constant [19]. Thus, combining Eq. (2) and supposing $\rho = 10$ Å, we obtain

$$\Delta E_b = 8.68 \times 10^{-4} n_{ring}/R \ (K_BT) \tag{8}$$

In Eq. (6), $n_{contact}$ denotes the contact number between walls of bundles, and then substituting Eq. (3) as well as $\rho = 10$ Å into Eq. (6), yields

$$E_{vdW} = -847.8R \times n_{contact} \ (K_BT) \tag{9}$$

Here, K_BT is the unit of the thermal energy.

Subsequently, based upon Eqs. (8) and (9), various sizes of nanotube rings may form if the total additive energy

$$E_{total} = \Delta E_b + E_{vdW} \tag{10}$$

is less than, or equal to, zero.

Thus in the following, based on our experimental results we can see that the model can provide the relation to length and diameter of original SWNT bundles with the resultant closed-ring structures. By means of SEM data, we can obtain the width δ and diameter D of the formed rings. Firstly, from δ, n_{ring} can be approximately derived with the model (the hexagonal close-packed structure for single SWNTs but not for the bundles). Secondly, according to the energy relationship $\Delta E_b + E_{vdW} = 0$ (for simplicity, not considering the negative situation), we can yield $n_{contact}$, the contact number between SWNT bundles. And again on the basis of the model, the number of SWNT bundles n_{bundle} in the ring's cross section and their radius ρ_{bundle} can be speculated accordingly. We can then analyze the matching between sizes of SWNT bundles and the detailed structures of the observed rings. Specifically, such properties as the width and diameter of the formed rings should match the original bundle size. By varying their sizes, we are expected to control the ultimate equilibrium ring structures.

Table 1
The number of SWNT bundles n_{bundle} and their approximate radius ρ_{bundle} as calculated based upon the supposed model (Fig. 3) and the energy relationship $\Delta E_b + E_{vdW} = 0$.

Requirements: $D(2R)$ and δ (nm)	n_{ring}	$n_{contact}$	n_{bundle}	ρ_{bundle} (nm)
300, 22	91	5	4	4.03
300, 30	169	7	5	5.00
500, 22	91	1	2	5.50
500, 30	169	3	3	7.50

Table 2
The number of SWNT bundles n_{bundle} and their approximate radius ρ_{bundle} as calculated from rarely larger SWNT rings.

Requirements: $D(2R)$ and δ (nm)	n_{ring}	$n_{contact}$	n_{bundle}	n_{bundle} (nm)
700, 22	91	0.76	1	11.0
700, 30	169	1.41	2	7.50
900, 22	91	0.46	1	11.0
900, 30	169	0.85	1	15.0

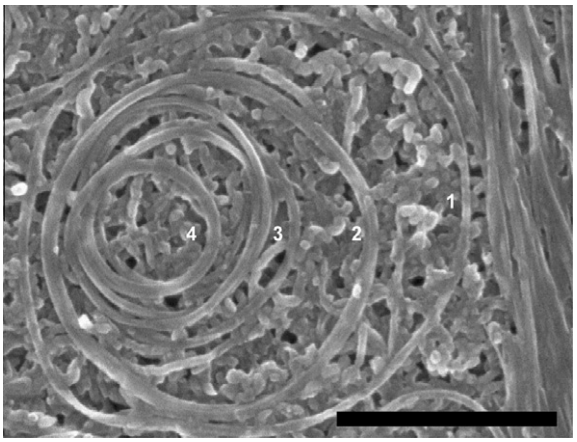

Fig. 4. SEM image of the multi ring structure formed from coarser and longer SWNT bundles, with clearly visible that the outermost ring has smaller width and the inner width is larger. Numbers from 1 to 4 mark different rings from outer to inner. The scale bar expresses 500 nm.

4. Results and discussion

In this section we will see that according to the above theory, we can finally reveal the internal properties of the present SWNT rings, and at the same time the resultant novel multi ring structures will also be well elucidated.

In our experiments, SWNT rings exist widely in many samples. The average diameter as determined by SEM is in range 200–500 nanometers (nm), and their width is concentrated in the range 20–30 nm. Therefore, we take representative diameters and width of them as examples (seeing Table 1). In this range, for the same ring diameter, the larger its width, the larger the component bundle radius will be. And conversely, for the same width, the bigger the ring diameter is, again a larger bundle radius will be obtained. The bundle radius ρ_{bundle} can signify the ring-forming feasibility (ρ_{bundle} cannot be less than the tube radius ρ and cannot be bigger than the ring width δ). So it can be seen that, according to the practical sizes of SWNT bundles, proper rings will be formed. For the same bundle radius ρ_{bundle}, the formed smaller rings' width δ will be wider than that of the corresponding bigger ones.

In addition, we can also find rings with larger radius. For this, the corresponding calculations have also been listed in Table 2. We can see that when the ring diameter is large enough, the values of $n_{contact}$ may be very small, or even less than one, therefore the ring width, δ, will be of smaller magnitude to $2\rho_{bundle}$. So usually, the width of bigger rings is comparatively smaller, consistent with the above analysis. As previously stated, the component SWNT bundles for larger rings will be coarser, which makes δ of them observed not too small. Moreover, we notice that $n_{contact}$ has decimal forms in Table 2, so is in Table 1 where only the integer part has been kept. We believe that decimal forms of $n_{contact}$ imply the multi-ring phenomenon, and the integer forms of them express the observed intact rings. The bundles possibly end up to form intact rings or to produce the multi ring structure. And the existence of such multi ring structures has universality (seeing Figs. 4–6).

As is shown in Fig. 4, there may be two or even more CNT bundles that move toward each other and assemble into the large-scale multi ring structure. The outermost ring has diameter ~931 nm and the width is ~19.8 nm. All the data are listed in Table 3. These values are shown to be in good agreement with the above theoretical analysis. Only the third one seems to be the exception, but it is not contradictory due to the uncertainty of sizes of real SWNT bundles. We therefore conclude two points as follows: 1. certain diameters of rings match appropriate width; 2. larger rings tend to have relatively smaller width. Again, Fig. 5 can further prove that bigger rings are likely to form multi ring structures and the smaller ones will easily be intact, as the former component

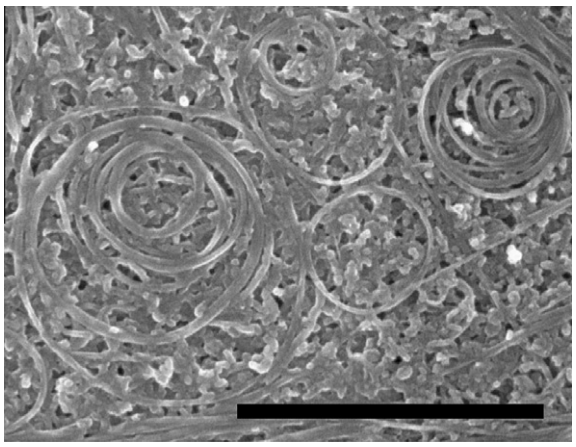

Fig. 5. SEM image of rings of SWNTs, showing bigger rings are likely in the form of multi ring structures and the smaller ones are easily intact. The scale bar expresses 1 μm.

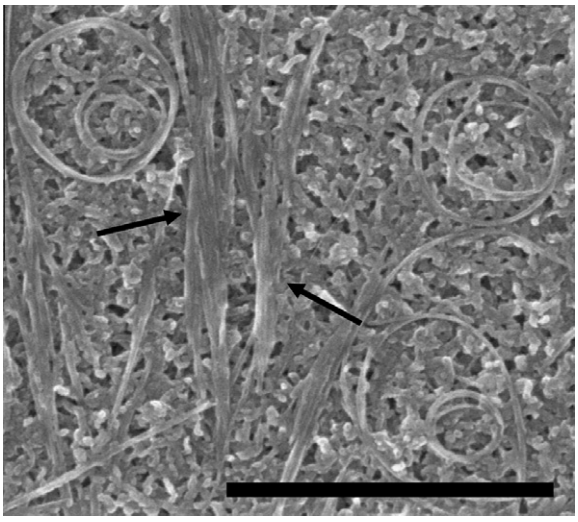

Fig. 6. SEM image of rings of SWNTs, showing that SWNTs or the bundles with different sizes will form different sizes of rings, as well as that coarse and short ones do not have the ability to form rings. The arrow pointed represents the most typical. The scale bar expresses 1 μm.

bundles are generally coarser and longer than the latter. And moreover, we should mention the fact that too coarse and short bundles may be unable to form rings (Fig. 6). In the picture, some thick and short bundles, with the natural extended state, are together in the gaps in rings, as they do not possess the ring-forming conditions. In short, we assume that either SWNTs or the bundles with different sizes will correspond to different forms of and different sizes of rings. Later, we will provide the relevant limit analysis.

We consider the smallest ring $2R$ = 100 nm and the biggest one $2R$ = 1000 nm, both of which are extremely rare in experiments. Similar to the previous discussion, requirements for SWNT bundles to form such rings are included in Table 4. In detail, if the circular diameter is very small (as 100 nm), the calculated original SWNT bundle will be very thin, or even near to the single SWNT, again consistent with the above mentioned. So referring to the practical nanotube system, there should be a minimum value for R (i.e. R_{min}). Coarser and shorter bundles will not self-fold into rings (seeing Fig. 6). Likewise on the contrary, for the very large circular diameter (as 1000 nm), this condition has also been considered, with the conclusion that the calculated $n_{contact}$ will be very small or even

Table 3
Diameters $D(2R)$ and width δ of SWNT rings respectively from 1 to 4 marked in Fig. 4.

Rings	$2R$ (nm)	δ (nm)
1	931	19.8
2	725	28.3
3	534	19.8
4	295	31.2

Table 4
The number of SWNT bundles n_{bundle} and their approximate radius ρ_{bundle} as calculated from limit situation to make further analysis.

Requirements: $D(2R)$ and δ (nm)	n_{ring}	$n_{contact}$	n_{bundle}	ρ_{bundle} (nm)
100, 10	19	7	5	1.67
100, 22	91	36	17	2.20–3.67
100, 30	169	69	32	2.14–3.00
1000, 10	19	0.0778	1	5.00
1000, 22	91	0.37	1	11.00
1000, 30	169	0.69	1	15.00

less than one, implying $2\rho_{bundle}$ will be equal to the ring width δ (i.e. δ_{min}). And the component bundles will be relatively thicker. So again according to the practical sizes of SWNT bundles, R should have a maximum value (i.e. R_{max}). The ring circumference $2\pi R_{max}$ should be less than or at most equal to the bundle length l_{bundle}. Overall, the macroscopic properties of the formed rings should match the component bundle size. The dimensions of ring structures will present a distribution in Fig. 7, where the medium sized rings will occur more frequently; neither too large nor too small rings will exist widely.

We have roughly predicted and proved the relationship between SWNT bundles and the ring structures. We make a conclusion that thinner bundles form small rings and the bigger ones are generally resulted from thicker bundles; the ring width should match its diameter, with relatively wider width for the smaller rings. However, due to the variety of dimensions of real SWNT bundles, some special cases indeed exist (i.e. the description to Fig. 4). Comparing the detailed conditions of theory and experiment is made difficult by the uncertainty of experimental systems and the experimenting processes. In the following, we have plotted a distribution chart, relating the ring width with the corresponding diameters, to further prove the above viewpoint.

The rough matching between the diameter and the width of SWNT rings has been presented in Fig. 7(a). The distribution chart was analyzed by counting the formed rings (about 100–200) taken from different areas of the sample using SEM. Again, we see that the larger rings have relatively smaller width and that the smaller ring tends to be a little wider. From Fig. 7(b), we can also see the existing predominance of the medium rings. Overall, the statistical data roughly reflect the general characteristics of the formed SWNT ring structures, excluding some allowable factors (i.e. drying, length limitation of the bundles, imperfection in the formed rings or the original bundles, etc.).

Previously, we have discussed the properties of nanotube rings from its energy conservation. But now, we divert to other means. As is shown in Fig. 8, entropic forces and statistical mechanics appear to play an important role in such various ring structures. That is to say, statistical theories of macromolecules may be useful for understanding the nanotubes' dynamic behavior and analyzing their interesting nanostructure formation. Even though, we will not give quantitative and detailed analysis about it, but instead to make discussions qualitative and macroscopical. Seeing Fig. 8, both of the compression of surrounding aligned SWNTs and the system entropy should be paid attention together. It is the compression of surrounding aligned SWNTs that makes SWNTs or the bundles have the chance to self-fold and then form rings or the

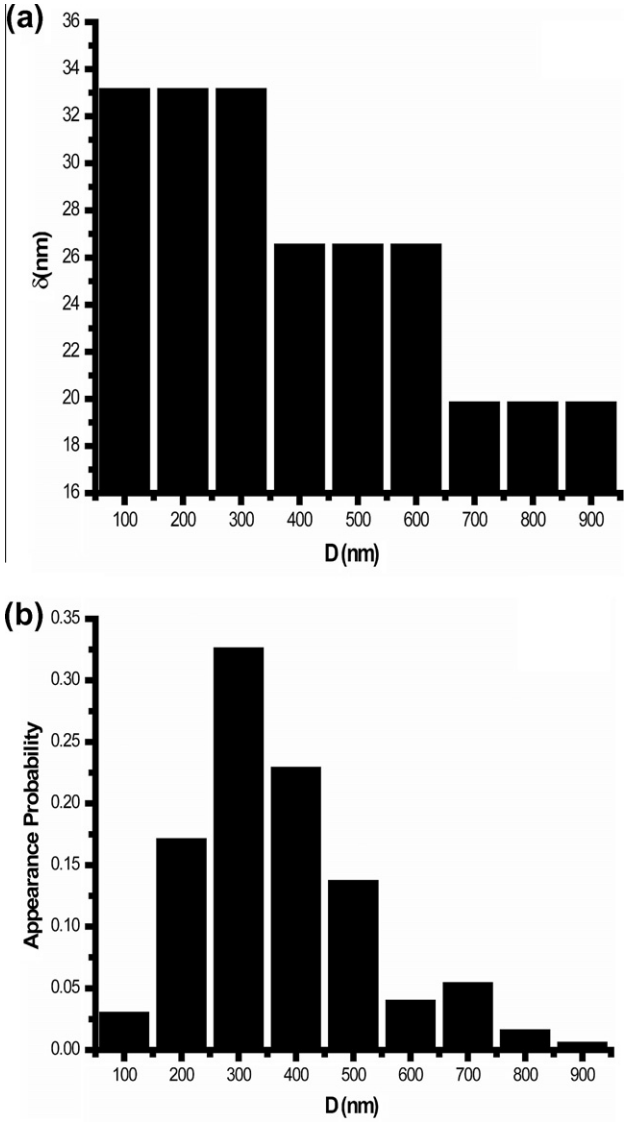

Fig. 7. Graph of the matching between the ring diameter D and its width δ, indicating δ decreases with D (a); and the distribution of appearance probability for different sizes of rings (b).

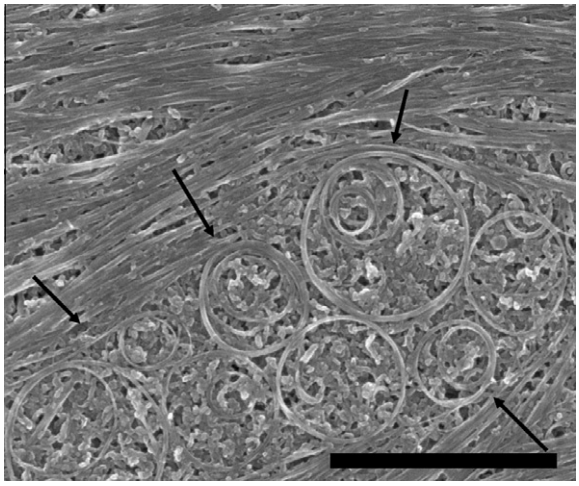

Fig. 8. SEM image of rings of SWNTs, revealing the driving effect for the ring-formation phenomenon may be from the compression of surrounding aligned SWNTs or from the inducement of system entropy. The arrow pointed represents the most typical. The scale bar expresses 1 μm.

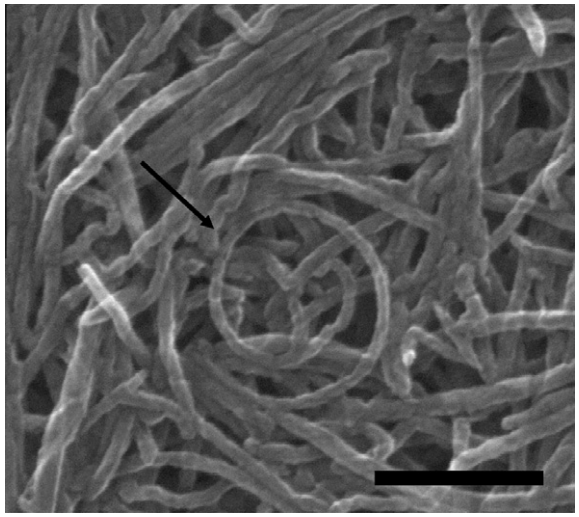

Fig. 9. SEM image of coils of MWNTs, revealing a process of coiling under the action of surrounding disordered nanotubes. The arrow pointed represents the coiled MWNT. The scale bar expresses 300 nm.

multi ring structures by the effects of system entropy. Another likely mechanism may involve the fact that the hydrophobic nanotubes acting as nuclei for bubble formation, can bend mechanically along the bubble–liquid interfaces, and ultimately keep the bending state with the bubbles collapsed [9]. Lastly, the end remained dangling bond during the acid oxidation treatment may prompt forming the closed nanotube ring structures as well, as eliminating these bonds will decrease the involved potential energy [10].

All in all, the above discussions have shed some light on the nature of SWNTs in self-organizing behavior. Thinner bundles have lower bending rigidity and greater flexibility than thicker ones, which makes them form different sizes of rings. The limited length and uneven diameters of realistic bundles also pose the reason that causes many of the phenomena of multi ring structures, or even some exceptions. Together with the above mentioned external factors, there are a number of issues related to the ring-forming exploration that need to be considered.

Complementarily, we should mention the behavior of multi-walled carbon nanotubes (MWNTs), which has been observed to be quite different because of their interlayer weak vdW interactions and the higher rigidity. Unlike SWNTs, MWNTs are difficult to link into rings. As is indicated in Fig. 9, they seem to form coils only with the help of surrounding environmental influences and without the contribution of attractive vdW interactions between different tubes or different parts of them at all (see the arrow-pointed MWNT). But this is not surprising. It has been proved that the toroidal forms of graphitic carbon tend to be chemically stable when defects of pentagons and heptagons are introduced into the original hexagonal networks, as they will allow the relaxation of the increased strain energy [3,20,21]. It is believed that any peculiar structures may form stably by combining pairs of pentagons (outer rim) and heptagons (inner rim). So from Fig. 9, we can also speculate that it is the defects on MWNT walls that promote forming the shown coil. Of course, the coiling might also originate from a number of other reasons, as is mentioned in the previous paragraph. However, here we emphasize the rare appearance of MWNT rings.

Finally, as previously stated, in the work, we have adopted the strain energies in bent SWNTs calculated by Zhou et al., who take account of the total energy of all the occupied band electrons. And then we have successfully explained the observed various nanotube ring

structures, showing the consistency between experiments and the involved theory. This continuum elastic theory has been proved to serve well to describe the nanotubes' forming into rings, and once again, the proper mechanical elastic model for nanotubes has been introduced and validated. And thereby, maybe we can further investigate the liquid crystalline self-assembling phenomenon in dispersions of SWNTs (seeing Fig. 1), for such liquid crystallinity is also believed to be related to nanotubes' inherent elastic properties, especially on the high Young's modulus E characterized mechanical elasticity.

5. Conclusions

The theoretical analysis presented in the paper was originated from calculating the formation energy of SWNT ring structures (E_{total}). Such qualitative and approximate tests broadly show their consistence with the observation in experiments. In the text, although we only consider the assumption $E_{\text{total}} = 0$ due to the purpose of theoretical quantification (it is difficult to apply the exact expression $E_{\text{total}} \leqslant 0$ to the current work), we have demonstrated that the work is indeed capable of providing reliable qualitative information about the equilibrium ring structures for SWNTs.

In summary, the wok is not that far removed from real systems. Based on sizes of original SWNT bundles, the formed circular diameter here is typically in the narrow range between 200 and 500 nm, with very few small or large rings observed. The proposed model and some approximate factors on it have successfully enabled testing of the current experimental observations. Even though it does not provide quite new physical insights and only the relatively limited amount of experimental results is reported, it is helpful to understand the interesting SWNT ring structures, an example for a recent trend in studying nano scale material phenomena, and further to provide some invaluable insights of nano-technology. As mentioned in the text, for example, many CNT-devices are sensitive to external mechanical loadings. So a proper understanding of the mechanics of CNTs will be crucial to rationally engineer its novel nano scale devices, and further to aid the development of theory about SWNT ring formation mechanism. If the forming details could be thoroughly understood, controlled, and optimized, we believe, they will become useful and fully exhibit the related specific characters. Thus, it will be very significant to further study such nanotube rings, and a broader investigation will be left to the future work.

Acknowledgments

We acknowledge discussions with Professor Graham Dawson to help improve the writing. This project is supported by the following foundations: National Science Foundation of China (10704051, 21143004), Suzhou Nano Special Project (ZXG0713), Special Foundation of President of The Chinese Academy of Science, Science and Technology Support Project of Jiangsu Province (BE2009643), and The National Basic Research Program of China (2010CB934700). And all of the SEM works were performed at the testing platform of Suzhou Institute of Nano-tech and Nano-bionics, Chinese Academy of Science.

References

[1] S. Ihara, S. Itoh, J. Kitakami, Phys. Rev. B 48 (1993) 5643.
[2] A.F. da Fonseca, D.S. Galv o, Phys. Rev. Lett. 92 (2004) 175502.
[3] Z.C. Ou-Yang, Z.B. Su, C.L. Wang, Phys. Rev. Lett. 78 (1997) 4055.
[4] M.J. Buehler, J. Mater. Res. 21 (2006) 2855.
[5] M.J. Buehler, Y. Kong, H. Gao, Y. Huang, J. Eng. Mater. Technol. 128 (2006) 3.
[6] M.J. Buehler, Y. Kong, H. Gao, J. Eng. Mater. Technol. 126 (2004) 245.
[7] Adam E. Cohen, L. Mahadevan, PNAS 100 (2003) 12141.
[8] M. Sano, A. Kamino, J. Okamura, S. Shinkai, Science 293 (2001) 1299.
[9] R. Martel, H.R. Shea, P. Avouris, Nature 398 (1999) 299.
[10] S. Itoh, S. Ihara, J. Kitakami, Phys. Rev. B 47 (1993) 1703.
[11] J. Liu, H. Dai, Jason H. Hafner, Daniel T. Colbert, Richard E. Smalley, Nature 385 (1997) 780.
[12] O. Hod, E. Rabani, R. Baer, Phys. Rev. B 67 (2003) 195408.
[13] L. Chen, H. Wang, J. Xu, X. Shen, L. Yao, L. Zhu, Z. Zeng, H. Zhang, H. Chen, J. Am. Chem. Soc. 133 (2011) 9654.
[14] V. Meunier, P. Lambin, A.A. Lucas, Phys. Rev. B 57 (1998) 14886.
[15] J. Yan, R. Kawamura, J.F. Marko, Phys. Rev. E 71 (2005) 61905.
[16] D.E. Hill, Y. Lin, A.M. Rao, L.F. Allard, Y.P. Sun, Macromolecules 35 (2002) 9466.
[17] X. Zhou, J.J. Zhou, Z.C. Ou-Yang, Phys. Rev. B 62 (2000) 13692.
[18] L.A. Girifalco, M. Hodak, R.S. Lee, Phys. Rev. B 62 (2000) 13104.
[19] A. Popescu, L.M. Woods, I.V. Bondarev, Phys. Rev. B 77 (2008) 115443.
[20] S. Itoh, S. Ihara, Phys. Rev. B 49 (1994) 13970.
[21] S. Itoh, S. Ihara, Phys. Rev. B 48 (1993) 8323.